Climate
of the Past

A 424-year tree-ring-based Palmer Drought Severity Index reconstruction of *Cedrus deodara* D. Don from the Hindu Kush range of Pakistan: linkages to ocean oscillations

Sarir Ahmad[1,2], **Liangjun Zhu**[1,2], **Sumaira Yasmeen**[1,2], **Yuandong Zhang**[3], **Zongshan Li**[4], **Sami Ullah**[5], **Shijie Han**[6], and **Xiaochun Wang**[1,2]

[1]Center for Ecological Research, Northeast Forestry University, Harbin 150040, China
[2]Key Laboratory of Sustainable Forest Ecosystem Management-Ministry of Education, School of Forestry, Northeast Forestry University, Harbin 150040, China
[3]Key Laboratory of Forest Ecology and Environment, State Forestry Administration, Institute of Forest Ecology, Environment and Protection, Chinese Academy of Forestry, Beijing 100091, China
[4]State Key Laboratory of Urban and Regional Ecology, Research Center for Eco-Environmental Sciences, Chinese Academy of Sciences, Beijing 100085, China
[5]Department of Forestry, Shaheed Benazir Bhutto University, Sheringal, Upper Dir 18000, Pakistan
[6]State Key Laboratory of Cotton Biology, School of Life Sciences, Henan University, Kaifeng 475001, China

Correspondence: Xiaochun Wang (wangx@nefu.edu.cn) and Shijie Han (hansj@iae.ac.cn)

Abstract. The rate of global warming has led to persistent drought. It is considered to be the preliminary factor affecting socioeconomic development under the background of the dynamic forecasting of the water supply and forest ecosystems in West Asia. However, long-term climate records in the semiarid Hindu Kush range are seriously lacking. Therefore, we developed a new tree-ring width chronology of *Cedrus deodara* spanning the period of 1537–2017. We reconstructed the March–August Palmer Drought Severity Index (PDSI) for the past 424 years, going back to 1593 CE. Our reconstruction featured nine dry periods (1593–1598, 1602–1608, 1631–1645, 1647–1660, 1756–1765, 1785–1800, 1870–1878, 1917–1923, and 1981–1995) and eight wet periods (1663–1675, 1687–1708, 1771–1773, 1806–1814, 1844–1852, 1932–1935, 1965–1969, and 1990–1999). This reconstruction is consistent with other dendroclimatic reconstructions in West Asia, thereby confirming its reliability. The multi-taper method and wavelet analysis revealed drought variability at periodicities of 2.1–2.4, 3.3, 6.0, 16.8, and 34.0–38.0 years. The drought patterns could be linked to the large-scale atmospheric–oceanic variability, such as the El Niño–Southern Oscillation, Atlantic Multi-decadal Oscillation, and solar activity. In terms of current climate conditions, our findings have important implications for developing drought-resistant policies in communities on the fringes of the Hindu Kush mountain range in northern Pakistan.

1 Introduction

Numerous studies have shown that the intensity and frequency of drought events have increased owing to rapid climate warming (IPCC, 2013; Trenberth et al., 2014). Droughts have serious adverse effects on social, natural, and economic systems (Ficklin et al., 2015; Yao and Chen, 2015; Tejedor et al., 2017; Yu et al., 2018). Globally, drought is considered to be the most destructive climate-related disaster, and it has caused billions of dollars in worldwide loss (van der Schrier et al., 2013; Lesk et al., 2016).

Pakistan has a semiarid climate, and its agricultural economy is vulnerable to drought (Kazmi et al., 2015; Miyan, 2015). The South Asian summer monsoon (SASM) is an integral component of the global climate system (Cook et al., 2010). Owing to the annually recurring nature of the SASM,

it is a significant source of moisture to the subcontinent and to surrounding areas such as northern Pakistan (Betzler et al., 2016). The active phase of the monsoon includes extreme precipitation in the form of floods and heavy snowfall, while the break phase mostly appears in the form of drought, thereby creating water scarcity. The active and break phases of the monsoon are also concurrent with the El Niño–Southern Oscillation (ENSO) and land–sea thermal contrast (Xu et al., 2018; Sinha et al., 2007, 2011). The large-scale variability in sea surface temperature (SST) is induced in the form of the Atlantic Multidecadal Oscillation (AMO), Pacific Decadal Oscillation (PDO), and some external forcing, i.e., volcanic eruption and greenhouse gases (Malik et al., 2017; Wei and Lohmann, 2012; Goodman et al., 2005).

The long-term drought from 1998 to 2002 reduced agricultural production, with the largest reduction in wheat, barley, and sorghum (from 60 % to 80 %) (Ahmad et al., 2004). Northern Pakistan is considered to contain the world's largest irrigation network (Treydte et al., 2006). The agricultural production and lives of local residents are strongly dependent on monsoon precipitation associated with large-scale oceanic and atmospheric circulation systems, including ENSO, AMO, PDO, and others (Treydte et al., 2006; Cook et al., 2010; Miyan, 2015; Zhu et al., 2017). However, the current warming rate has changed the regional hydrological conditions, thereby leading to an unsustainable water supply (Hellmann et al., 2016; Wang et al., 2017). It is not only critical for agricultural production, but also leads to forest mortality, vegetation loss (Martínez-Vilalta and Lloret, 2016), and increased risk of wildfires (Abatzoglou and Williams, 2016). The degradation of grasslands and loss of livestock caused by drought affect the lifestyle of nomadic peoples, especially in high-altitude forested areas (Pepin et al., 2015; Shi et al., 2019).

The Hindu Kush Himalayan region (HKH) is the source of 10 major rivers in Asia, which provide water resources for 20 % of the world's population (Rasul, 2014; Bajracharya et al., 2018). The region is particularly prone to droughts, floods, avalanches, and landslides, with more than 1 billion people being exposed to increasingly frequent and serious risks of natural disasters (Immerzeel et al., 2010, 2013). The extent of climate change in this area is significantly higher than the world average, which has seriously threatened the safety of life and property, traffic, and other infrastructure in the downstream and surrounding areas (Lutz et al., 2014). Dry conditions have been exacerbated by an increase in the frequency of heat waves in recent decades (Immerzeel et al., 2010; IPCC, 2013). The trends in the intensity and frequency of drought are very complex in the HKH, and there is no clear measuring tool to compute how long drought might persist. Climate uncertainty complicates the situation, for example in terms of whether the drought trend is increasing or decreasing (Chen et al., 2019). Most studies suggest that the wetting trend in the HKH will continue in the coming decades (Treydte et al., 2006). However, some extreme drought events in

the region have been very serious and persistent (Gaire et al., 2017). Little has been done to examine the linkage between drought trends and large-scale oceanic climate drivers (Cook et al., 2003; Gaire et al., 2017). In northern Pakistan, instrumental climate records are inadequate in terms of quality and longevity (Treydte et al., 2006; Khan et al., 2019).

In high-altitude, arid, and semiarid areas, forest growth is more sensitive to climate change, so it is necessary to understand the past long-term drought regimes (Wang et al., 2008). Climate reconstruction is the best way to understand long-term climate change and expand the climate record to develop forest management strategies. Researchers have used multiple proxies, including ice cores, speleothems, lake sediments, historical documents, and tree rings, to reconstruct past short-term and long-term climate change. In addition, tree rings are widely used in long-term paleoclimatic reconstructions and future climate forecasting (Liu et al., 2004) because of their accurate dating, high resolution, wide distribution, easy access, long time series, and abundant environmental information (Esper et al., 2016; Zhang et al., 2015; Klippel et al., 2017; Shi et al., 2018; Chen et al., 2019)

Before 2000, there are few tree-ring studies in Pakistan. Bilham et al. (1983) found that tree rings of juniper trees from the Sir Sar range in the Karakoram have the potential to reconstruct past climate. Esper et al. (1995) developed a 1000-year tree-ring chronology at the timberline of Karakorum and found that temperature and rainfall are both controlling factors for juniper growth. More juniper tree-ring chronologies were developed at the upper timberline in the Karakorum (Esper, 2000; Esper et al., 2001, 2002). *Abies pindrow* and *Picea smithiana* were also used for dendroclimatic investigation in Pakistan (Ahmed et al., 2009, 2010a). Recently, more studies on tree rings have been carried out in Pakistan (Ahmed et al., 2010b, 2011a; Khan et al., 2013; Akbar et al., 2014; Asad et al., 2017a, b, 2018), but few have used tree rings to reconstruct the past climate, especially the drought index.

In this study, we collected drought-sensitive tree-ring cores of *Cedrus deodara* from the upper and lower HKH of Pakistan. These tree rings have good potential for dendroclimatic studies (Yadav, 2013). Then, the March–August Palmer Drought Severity Index (PDSI) was reconstructed for the past 424 years to examine the climatic variability and driving forces. To verify its reliability, we compared our reconstructed PDSI with other available paleoclimatic records (Treydte et al., 2006) near our research area. The intensity and drought mechanisms in this area were also discussed. This is the first time that the drought index has been reconstructed in northern Pakistan, and the study can be used as a baseline for further tree-ring reconstructions in Pakistan.
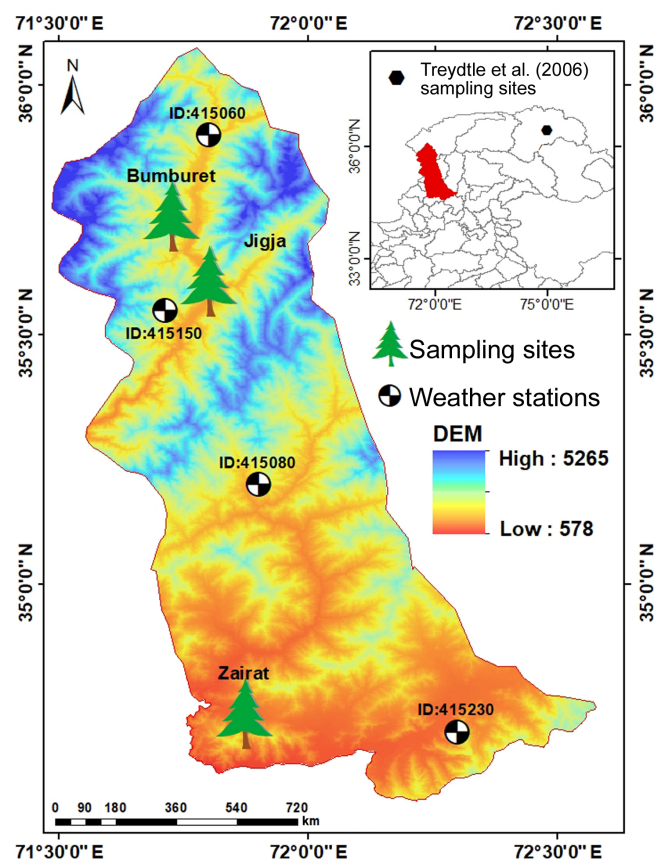
Figure 1. Map of the weather stations (Drosh station) and sampling sites in the Chitral, Hindu Kush mountains, Pakistan. Different colors represent the elevation changes in the study area.

2 Material and methods

2.1 Study area

We conducted our research in the Hindu Kush (HK) mountain range of northern Pakistan (35.36° N, 71.48° E; Fig. 1). Northern Pakistan has a subtropical monsoon climate. Summer is dry and hot, spring is wet and warm, and at some high altitudes, it snows year-round. March is the wettest month (with average precipitation of 107.0 mm), while July or August is the driest (with average precipitation of 6.3 mm). July is the hottest month (mean monthly temperature of 36.0 °C) and January is the coldest (mean monthly temperature of −0.8 °C) (Fig. 2).

The elevation of the study area ranges from 1070 to 7708 m, with an average elevation of 3500 m. The sampled Jigja site is located on the east slope of the mountain. The stand density is relatively uniform with the dominant species. Among the tree species, *Cedrus deodara* is the most abundant, with 156 individuals per square hectometer and a basal area of 27 m² hm⁻². The Chitral forest is mainly composed of *C. deodara*, *Juglans regia*, *Juniperus excelsa*, *Quercus incana*, *Quercus dilatata*, *Quercus baloot*, and *Pinus wallichi-*

ana. C. deodara was selected for sampling because of its high dendroclimatic value (Khan et al., 2013). The soil at our sampling sites was acidic, with little variation within a stand of forest. Similarly, the soil water-holding capacity ranged from 47 % ± 2.4 % to 62 % ± 4.6 %, while the soil moisture ranged from 28 % ± 0.57 % to 57 % ± 0.49 % (Khan et al., 2010).

Climate data such as monthly precipitation and temperature (1965–2016) were obtained from the meteorological station of Drosh in northern Pakistan. The PDSI was downloaded from data sets of the nearest grid point (35.36° N, 71.48° E) through the Climatic Research Unit (CRU TS.3.22; 0.5° latitude × 0.5° longitude). The most common reliable period spanning from 1965 to 2016 was used (http://climexp. knmi.nl/, last access: 24 April 2020) for dendroclimatic studies (Harris et al., 2014; Shekhar, 2015).

The AMO index was downloaded from the KNMI Climate Explorer (https://climexp.knmi.nl/getindices. cgi?WMO=UKMOData/amo_hadsst&STATION= AMO_hadsst&TYPE=i&id=someone@somewhere, last access: 24 April 2020) (van Oldenburg, 2009). The reconstructed June–August SASM data were downloaded from the Monsoon Asia Drought Atlas (http://drought.memphis.edu/MADA, last access: 24 April 2020) over the period of 1300–2005.

2.2 Tree-ring collection and chronology development

Tree-ring cores were collected in the Chitral forest from *C. deodara* trees. To maintain the maximum climatic signals contained in the tree rings, undisturbed open canopy trees were selected. One core per tree at breast height (approximately 1.3 m above the ground) was sampled using a 5.15 mm diameter increment borer (Haglöf, Sweden; Långsele, Sweden). In addition, several ring-width series were also downloaded from the International Tree-Ring Data Bank for the Bumburet forest and Ziarat forest (https://www. ncdc.noaa.gov/paleo-search/, last access: 24 April 2020) collected in 2006 (Fig. 1).

All the tree-ring samples were first glued and then progressively mounted, dried, and polished according to a set procedure (Fritts, 1976; Cook and Kairiukstis, 1990). The calendar year of each ring was assigned and properly cross-dated. False rings were identified using a skeleton plot and crossdated, as mentioned in Stokes and Smiley (1968).

The cores were measured using the semiautomatic Velmex measuring system (Velmex, Inc., Bloomfield, NY, USA) with an accuracy of 0.001 mm. The COFECHA program was then used to check the accuracy of the cross-dating and measurements (Holmes, 1983). All false measurements were modified, and the cores that did not match the master chronology were not used to develop the tree-ring chronology. The synthesized tree-ring width chronology (Fig. 3) was built using the R program (Zang and Biondi, 2015). To preserve climate signals and avoid noise, appropriate detrending was
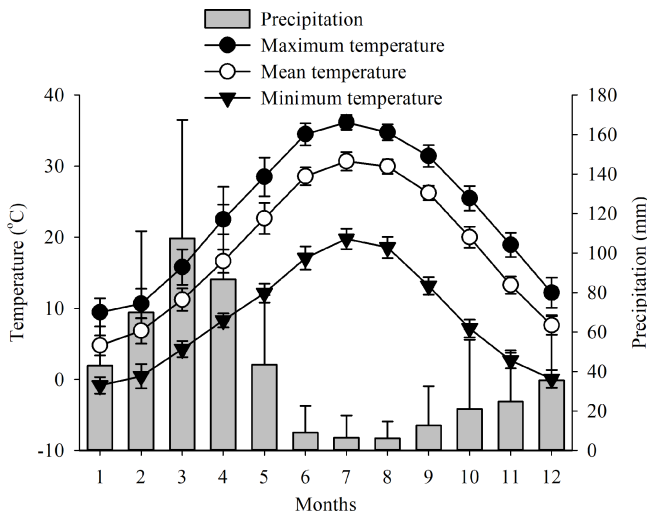
Figure 2. Monthly maximum, mean, and minimum temperature (°C) as well as total precipitation (mm) at the Drosh weather station (35.07° N, 71.78° E; 1465 m), Pakistan (1965–2013).

introduced. Biological trends in tree growth associated with tree age were conservatively detrended by fitting negative exponential curves or linear lines (Fritts, 1976). The tree-ring chronology was truncated where the expressed population signal (EPS) was larger than 0.85, which is a generally accepted standard for more reliable and potential climate signal results (Wigley et al., 1984; Cook and Kairiukstis, 1990). The mean correlation between trees (Rbar), mean sensitivity (MS), and EPS were calculated to evaluate the quality of the chronology (Fritts, 1976). Higher MS and EPS values indicated a strong response to climate change (Cook and Kairiukstis, 1990).

2.3 Statistical analysis

Correlation analysis was conducted between the tree-ring index (TRI) and monthly temperature, precipitation, and PDSI (from the previous June to the current September; collected from nearby stations or downloaded from the KNMI). Then, the PDSI was reconstructed according to the relationship between the TRI and climate variables. To test the validity and reliability of our model, the reconstruction was checked by split-period calibration and verification methods subjected to different statistical parameters, including reduction of error (RE), coefficient of efficiency (CE), Pearson correlation coefficient (r), R squared (R^2), product means test (PMT), sign test (ST), and Durbin–Watson test (DWT) (Fritts, 1976). The RE and CE have a theoretical range of $-\infty$ to $+1$, but the benchmark for determining skill is the calibration and verification period mean. Therefore, RE >0 and CE >0 indicate reconstruction skill in excess of climatology (Cook et al., 1999). The PMT is used to test the level of consistency between the actual and estimated values considering the signs

and magnitudes of departures from the calibration average (Fritts, 1976). The ST expresses the coherence between reconstructed and instrumental climate data by calculating the number of coherence and incoherence values, which was often used in previous studies (Fritts, 1976; Cook et al., 2010). The DWT is used to calculate first-order autocorrelation or linear trends in regression residuals (Wiles et al., 2015). RE and CE values larger than zero are considered skills (Fritts, 1976; Cook et al., 1999).

According to Chen et al. (2019), we defined the wet or dry years of our reconstruction with a PDSI value greater than or less than the mean ± 1 standard deviation. The mean ± 1 standard deviation is an easy method to calculate the dry and wet years, which has been observed in different tree-ring PDSI reconstructions (Wang et al., 2008; Chen et al., 2019). We assessed the dry and wet periods for many years based on strength and intensity.

Although there were few reconstructions in our study area, we compared our reconstruction with other available drought reconstructions near the study area (Treydte et al., 2006). The multi-taper method (MTM) was used for spectral analysis, and wavelet analysis was used to determine the statistical significance of band-limited signals embedded in red noise by providing very high-resolution spectral estimates that eventually provided the best possible option against leakage. To identify the local climate change cycle, the background spectrum was used (Mann and Lees, 1996).

3 Results

3.1 Main climate-limiting factors for *Cedrus deodar*

The statistical parameters of the tree-ring chronologies, including MS (0.16), Rbar (0.59), and EPS (0.94), indicated that there were enough common signals in our sampled cores and that our chronology was suitable for dendroclimatic studies. According to the threshold of EPS (EPS >0.85), 1593–2016 was selected as the reconstruction period to truncate the period of 1537–1593 of the chronology (Fig. 3).

The TRI was significantly positively correlated with the monthly PDSI ($p<0.01$) (Fig. 4a). However, the TRI was positively correlated with the precipitation in October of the previous year and February–May of the current year; it was negatively correlated with the precipitation in September of the previous year ($p<0.001$). The TRI was significantly positively correlated ($p<0.001$) with the minimum temperature in September and December of the previous year and January and February of the current year (Fig. 4b). Similarly, the TRI was significantly negatively correlated ($p<0.001$) with the maximum temperature in January, October, and December of the previous year and February–June of the current year. The TRI was only significantly positively correlated with the maximum temperature in September (Fig. 4b).
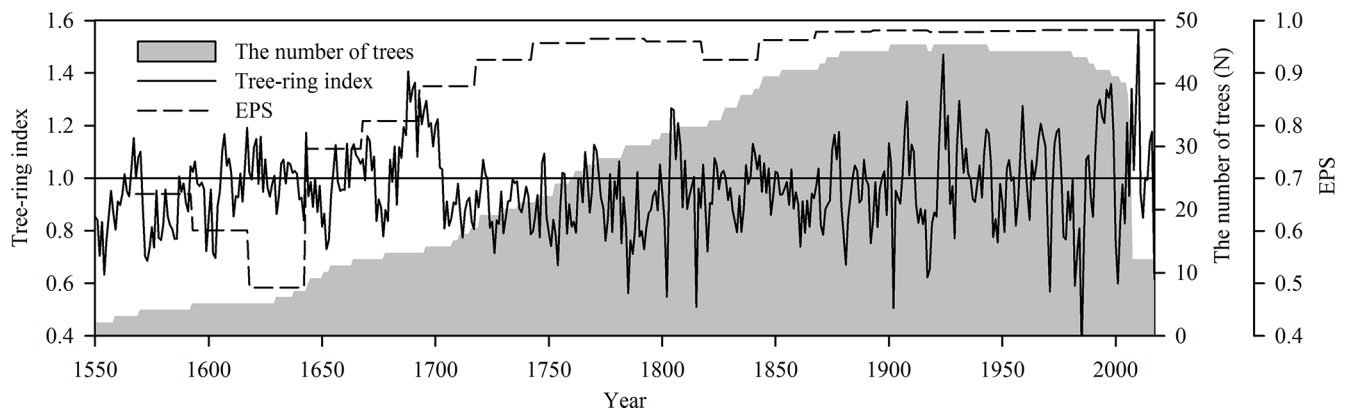
Figure 3. The regional tree-ring width chronology from 1550 to 2017 in the Chitral, Hindu Kush mountains, Pakistan. The gray area represents the sample depth.
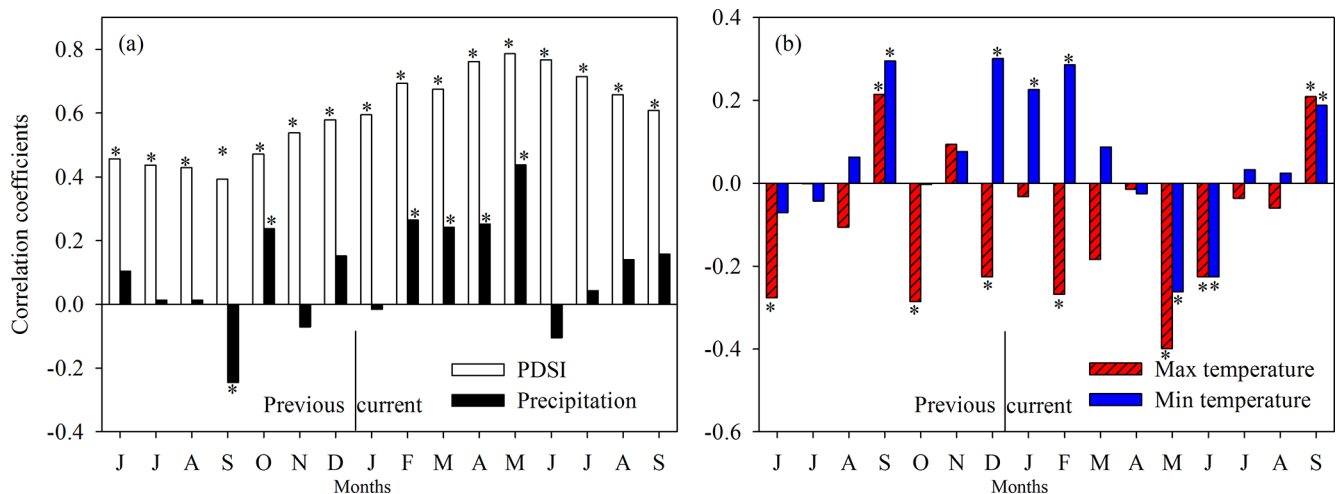

Figure 4. Pearson correlation coefficients between the tree-ring index of *C. deodara* and the monthly total precipitation (1965–2013), scPDSI (1960–2013) **(a)**, monthly maximum, and minimum temperature (1965–2013) **(b)** from June of the previous year to September of the current year. Significant correlations ($p < 0.05$) are denoted by asterisks. "Previous" and "current" represent the previous and current year, respectively.

3.2 Reconstruction of past drought variation in northern Pakistan

The correlation between the PDSI and the TRI was the highest from March to August, thereby indicating that the growth of *C. deodara* was most strongly affected by drought before and during the growing season. Based on the above correlation analysis results, the March–August PDSI was the most suitable for seasonal reconstruction. The linear regression model between the TRI and mean March–August PDSI for the calibration period from 1960 to 2016 was significant ($F = 52.4$; $p < 0.001$; adjusted $R^2 = 0.49$; $r = 0.70$). The regression model was as follows:

$$Y = 5.1879x - 5.676,$$

where Y is the mean March–August PDSI and x is the TRI.

The split calibration–verification test showed that the explained variance was higher during the two calibration periods (1960–1988 and 1989–2016). For the calibration period of 1960–2016, the reconstruction accounted for 49.2 % of the self-calibrating Palmer Drought Severity Index (scPDSI) variation (49 % after accounting for the loss of degrees of freedom). The statistics of R, R^2, ST, and PMT were all significant at $p < 0.05$, thereby indicating that the model was reliable (Table 1). Here, the most rigorous RE and CE tests in the verification period were all positive. Thus, these results made the model clearer and more robust in the PDSI reconstruction.

The instrumental and reconstructed PDSIs of the HK mountains had similar trends and parallel calibrations during short-term and long-term scales in the 20th century (Fig. 5a).

Table 1. Statistical test for the tree-ring reconstruction of the March–August PDSI in the Chitral Hindu Kush range of northern Pakistan based on a split calibration–verification procedure.

Calibrations	r	R^2	Verification	RE	CE	ST	DW	RMSE	PMT
1960–2016	0.70	0.49	–	0.44	–	(43, 14)*	1.06*	1.21	10.0*
1989–2016	0.82	0.67	1960–1988	0.61	0.62	(23, 6)*	1.0*	1.72	5.80*
1960–1988	0.73	0.53	1989–2016	0.64	0.62	(24, 4)*	0.98*	1.56	7.42*

* The asterisks represent the significance at the 95 % confidence level ($p < 0.05$), RE: reduction of error, CE: coefficient of efficiency, ST: sign test, DW: Durbin–Watson test, RMSE: root mean square error, PMT: product means test.

However, the reconstructed scPDSI did not fully capture the magnitude of extremely dry or wet conditions.

3.3 Drought regime in the Hindu Kush mountain range, northern Pakistan, for the past 424 years

The dry periods were recorded as 1593–1598, 1602–1608, 1631–1645, 1647–1660, 1756–1765, 1785–1800, 1870–1878, 1917–1923, and 1981–1995. Similarly, the wet periods were recorded as 1663–1675, 1687–1708, 1771–1173, 1806–1814, 1844–1852, 1932–1935, 1965–1969, and 1996–2003 (Fig. 5b).

To verify the accuracy and reliability of our reconstruction, we compared our results with the nearby precipitation reconstruction of Treydte et al. (2006) (Fig. 6). In the reconstruction of Treydte et al. (2006), the high and low raw $\delta^{18}O$ values represent dry and wet conditions, respectively, which is opposite to the PDSI. In most periods, our PDSI reconstruction and the precipitation reconstruction of Treydte et al. (2006) showed good consistency (Fig. 6). However, in some periods, they also showed inconsistent or even opposite changes in drought reconstruction. For example, in 1865–1900, the reconstruction of Treydte et al. (2006) was very wet, while our reconstruction was normal. In the periods of 1800–1810 and 1694–1702, the reconstruction of Treydte et al. (2006) was very dry, but our reconstruction was wet (Fig. 6).

Spectral analysis of the historical PDSI changes in the HK mountains showed several significant changes (95 % or 99 % confidence level), with periods of 33.0–38.0 (99 %), 16.8 (99 %), and 2.0–3.0 (99 %) corresponding to significant periodic peaks (Fig. 7).

The spatial correlation analysis between our reconstructed PDSI and the actual PDSI from May to August showed that our drought reconstruction was a good regional representation (Fig. 8). This showed that our reconstruction was reliable and could reflect the drought situation in the region. In addition, the PDSI for the low-frequency (the 31-year moving average) reconstruction had good consistency with the AMO ($r = 0.53$; $p < 0.001$; 1890–2001) and SASM ($r = 0.35$; $p < 0.001$; 1608–1990), which indicated that these are the potential factors affecting the drought patterns in the region (Fig. 9).

4 Discussion

4.1 Drought variation in the Hindu Kush range of Pakistan

The growth–climate relationship revealed the positive and negative influences of precipitation and summer temperature on growth. It indicated that water availability (PDSI) is the main limiting factor affecting the growth of *C. deodara*. Singh et al. (2006) reported that precipitation in the previous October limits the growth of *C. deodara*, while Ahmed et al. (2011b) found no such effect. Except for the previous August and November and the current September, maximum temperature had a negative impact on the growth of *C. deodara*, while the minimum temperature did not. These results suggest that moisture conditions in April–July are critical to the growth of *C. deodara* in the study area (Borgaonkar et al., 1996; Khan et al., 2013). Chitral does not receive monsoon rains, which is why it is difficult to understand how trees respond to different moisture trends.

Here, we developed a 468-year (1550–2017) tree-ring chronology of *C. deodara* and reconstructed the 424-year (1593–2016) drought variability of the HK range in northern Pakistan. The peak years (narrow rings), namely 2002, 2001, 2000, 1999, 1985, 1971, 1962, 1952, 1945, 1921, 1917, 1902, and 1892, were recorded in our tree-ring record. Narrow ring formation occurs when extreme drought stress reduces cell division (Fritts et al., 1976; Shi et al., 2014). Therefore, the narrow rings were also consistent with the extreme drought years. Among them, 2001, 1999, 1952, and 1921 were identified by previous studies (Esper et al., 2003; Ahmed et al., 2010a; Zafar et al., 2010; Khan et al., 2013; He et al., 2018). Sigdel and Ikeda (2010) reported that droughts occurred in 1974, 1977, 1985, 1993, the winter of 2001, and the summers of 1977, 1982, 1991, and 1992. Our PDSI reconstruction fully captured the widespread drought in Pakistan, Afghanistan, and Tajikistan during 1970–1971 (Yu et al., 2014). The above drought disrupted daily life and led to food and water shortages and livestock losses in high-altitude areas (Yadav, 2011; Yadav and Bhutiyani, 2013; Yadav et al., 2017). This drought might have also been due to the failure of western disturbance precipitation (Hoerling et al., 2003). Similarly, the 17 wettest years were observed from wide rings in 2010, 2009, 2007, 1998, 1997, 1996, 1993, 1931,
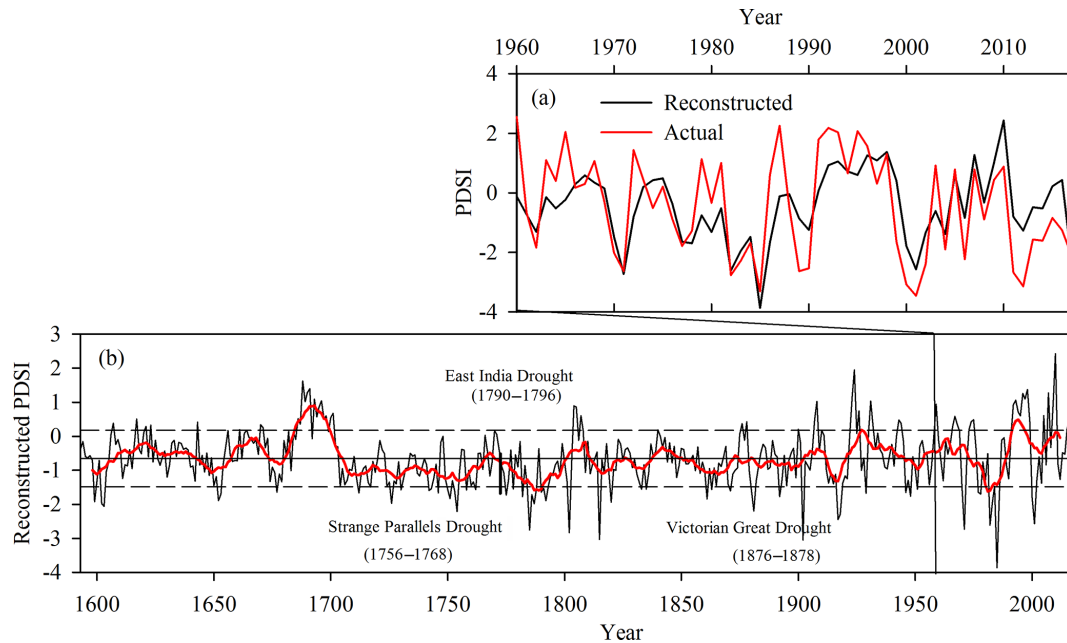
Figure 5. The scPDSI reconstruction in the Chitral Hindu Kush mountains, Pakistan. **(a)** Comparison between the reconstructed (black line) and actual (red line) scPDSI; **(b)** the variation of the annual (black solid line) and 11-year moving average (red bold line) Mar–Aug scPDSI from 1593 to 2016 with the mean value ± 1 standard deviation (black dashed lines).
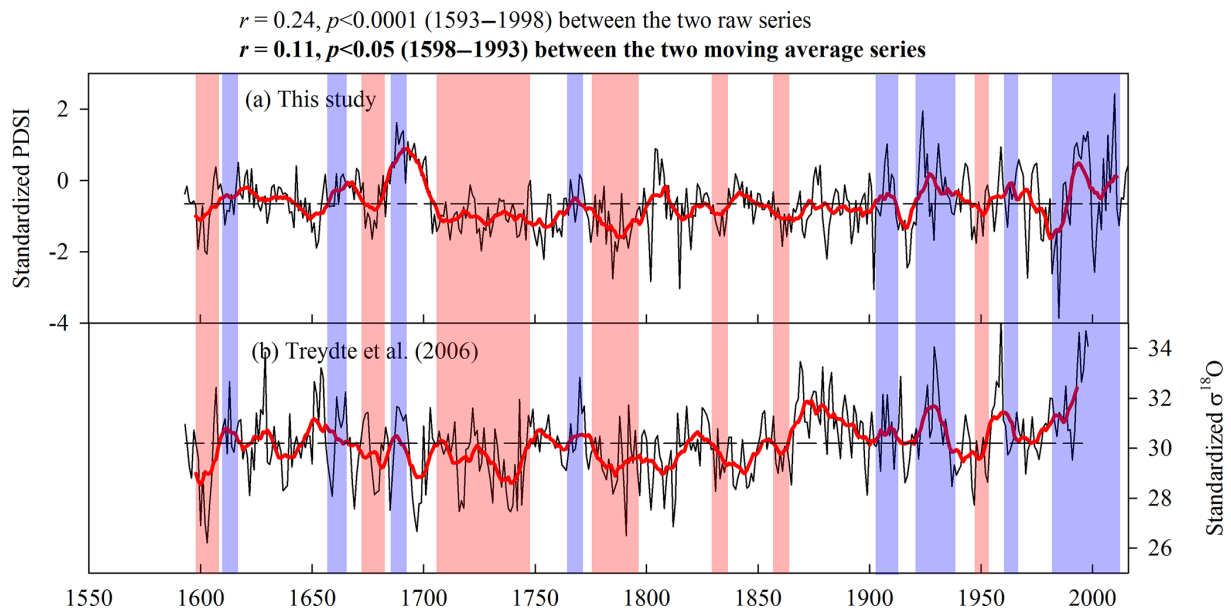

Figure 6. Comparison of our PDSI reconstruction **(a)** with the precipitation reconstruction (reversed tree-ring δ^{18}O) of Treydte et al. (2006) **(b)** in northern Pakistan. Purple and brown shaded areas represent the consistent wet and dry periods in the two reconstructions, respectively. The two correlation coefficients ($r = 0.24$ and $r = 0.11$) are the correlations of two original annual-resolution reconstruction series and two 11-year moving average series, respectively.

1924, 1923, 1908, 1696, 1693, 1691, 1690, 1689, and 1688. The floods of July 2010 were also captured by our reconstruction, which affected approximately 20 % of Pakistan (20 million people) (Yaqub et al., 2015). The wet years of 1997, 1996, 1993, 1696, 1693, 1691, 1690, 1689, and 1688 were in

agreement with the results of Khan et al. (2019). Similarly, the wet years of 1923, 1924, 1988, 2007, 2009, and 2010 coincided with the reconstruction of Chen et al. (2019).

As shown in Fig. 5, the mean of our reconstructed PDSI was below zero. There are two possible reasons for this phe-
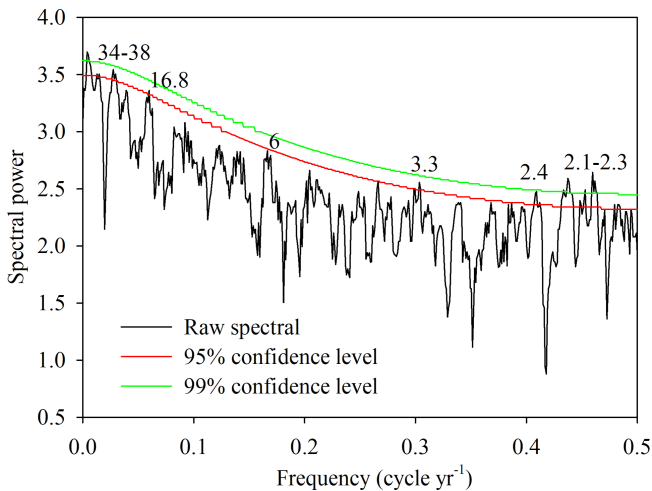
Figure 7. The multi-taper method spectrums of the reconstructed scPDSI from 1593 to 2016. The red and green line represent the 95 % and 99 % confidence level, respectively. The figures above the significance line represent significant periods of drought at the 95 % confidence level.

nomenon. First, tree growth is more sensitive to drying than to wetting. As a result, more drought information is recorded in ring widths. This leads to a drier (less than zero) PDSI reconstructed with tree rings. This phenomenon exists in many tree-ring PDSI reconstructions (Hartl-Meier et al., 2017; Wang et al., 2008). Second, the period (1960–2016) used to reconstruct the equation was relatively dry. This caused the mean of the reconstruction equation to be lower than zero (dry), thereby resulting in lower values for the whole reconstruction. Therefore, when applying the PDSI data reconstructed by tree rings, its relative value is relatively reliable, and the absolute value data can only be used after adjustment. The adjustment method for the absolute value needs to be further studied.

Our reconstruction also captured a range of changes in climate mentioned in other studies (Ahmad et al., 2004; Yu et al., 2014; Chen et al., 2019; Gaire et al., 2019). Our reconstruction featured nine dry periods (1593–1598, 1602–1608, 1631–1645, 1647–1660, 1756–1765, 1785–1800, 1870–1878, 1917–1923, and 1981–1995) and eight wet periods (1663–1675, 1687–1708, 1771–1773, 1806–1814, 1844–1852, 1932–1935, 1965–1969, and 1990–1999). The dry periods of 1598–1612, 1638–1654, 1753–1761, 1777–1793, and 1960–1985 and the wet periods of 1655–1672, 1681–1696, 1933–1959, and 1762–1776 coincided with those reconstructed by Chen et al. (2019) in northern Tajikistan. The most serious droughts in 1871, 1881, and 1931, and the short-term drought from 2000 to 2002 mentioned by Ahmad et al. (2004), were also found to be very dry in our reconstruction.

The dry period of 1645–1631 is also reflected in the tree-ring-based drought variability of the Silk Road (Yu et al.,

2014). Three mega-drought events in Asian history (Yadav, 2013; Panthi et al., 2017; Gaire et al., 2019), namely the Strange Parallels Drought (1756–1768), East India Drought (1790–1796), and Late Victorian Great Drought (1876–1878), were clearly recorded in our reconstructed PDSI. This could mean that widespread drought on the continent could be linked to volcanic eruptions (Chen et al., 2019). The wet period of 1995–2016 was very consistent with that of Yadav et al. (2017). These results suggest that the long-term continuous wet periods in 31 years out of the past 576 years (1984–2014) might have increased the mass of glaciers in the northwest Himalaya and Karakoram mountains (Cannon et al., 2015). Therefore, we speculate that the size of the HK glacier and the mass of glaciers near our study areas will continue to increase if the wet trend continues.

Our PDSI reconstruction and the precipitation reconstruction of Treydte et al. (2006) show a strong consistency (Fig. 6), which proves that our reconstruction is reliable. The discrepancies in some periods might have been because the PDSI is affected by temperature and may not be completely consistent with precipitation (Li et al., 2015). The inconsistency between the reconstruction of ring widths and oxygen isotopes in some periods might also have been due to the different responses of radial growth and isotopes to disturbance (McDowell et al., 2002).

To test the consistency of the drought period, we compared this reconstruction with other drought and precipitation records based on tree-ring reconstructions in central Eurasia and China, which were adjacent to our study area, but none of them are completely matched. The dry periods of our reconstruction are similar to some periods of the reconstruction by Sun and Liu (2019) in 1629–1645 and 1919–1933. However, we found that our drought periods are more consistent with the drought periods of the May–June reconstruction in the south–central Tibetan Plateau (He et al., 2018), such as 1593–1598 (1580–1598), 1647–1660 (1650–1691), 1785–1800 (1782–1807), and 1870–1878 (1867–1982). This difference may be due to differences in geographical location, species, and reconstruction indices, among others (Gaire et al., 2019). In addition, the lack of consistency between different data sets or regions might have been due to the dominance of internal climate variability over the impact of natural exogenous forcing conditions on multidecadal timescales (Bothe et al., 2019).

4.2 Linkage of drought variation with ocean oscillations

The results of wavelet and MTM analysis indicated that the low- and high-frequency periods of drought in northern Pakistan may have a teleconnection with both large- and small-scale climate oscillations (Fig. 7). The high frequency of the drought cycle (2.1–3.3 years) may be related to ENSO (van Oldenborgh and Burgers, 2005). The ENSO index in different equatorial Pacific regions has a significant positive correlation with our reconstructed drought index, with a lag of
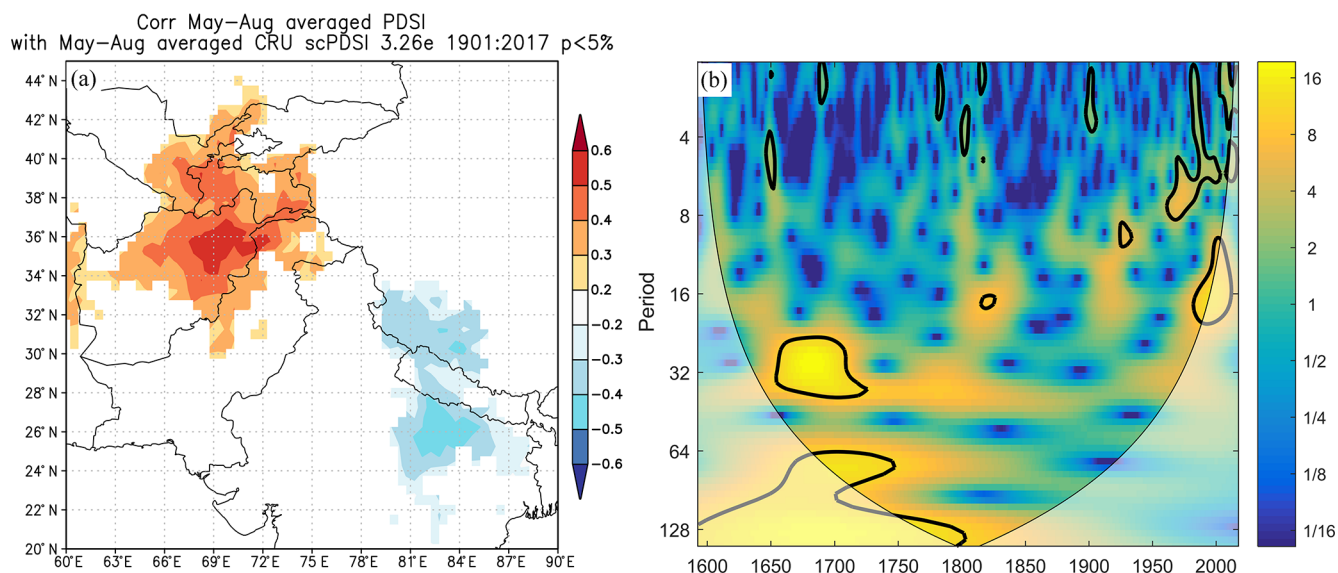
Figure 8. (a) Spatial correlation between the actual May–August PDSI and the reconstructed May–August scPDSI (1901–2017). **(b)** The wavelet analysis of the reconstructed scPDSI in the Chitral Hindu Kush ranges, Pakistan. The 95 % significance level against red noise is shown as a black contour.
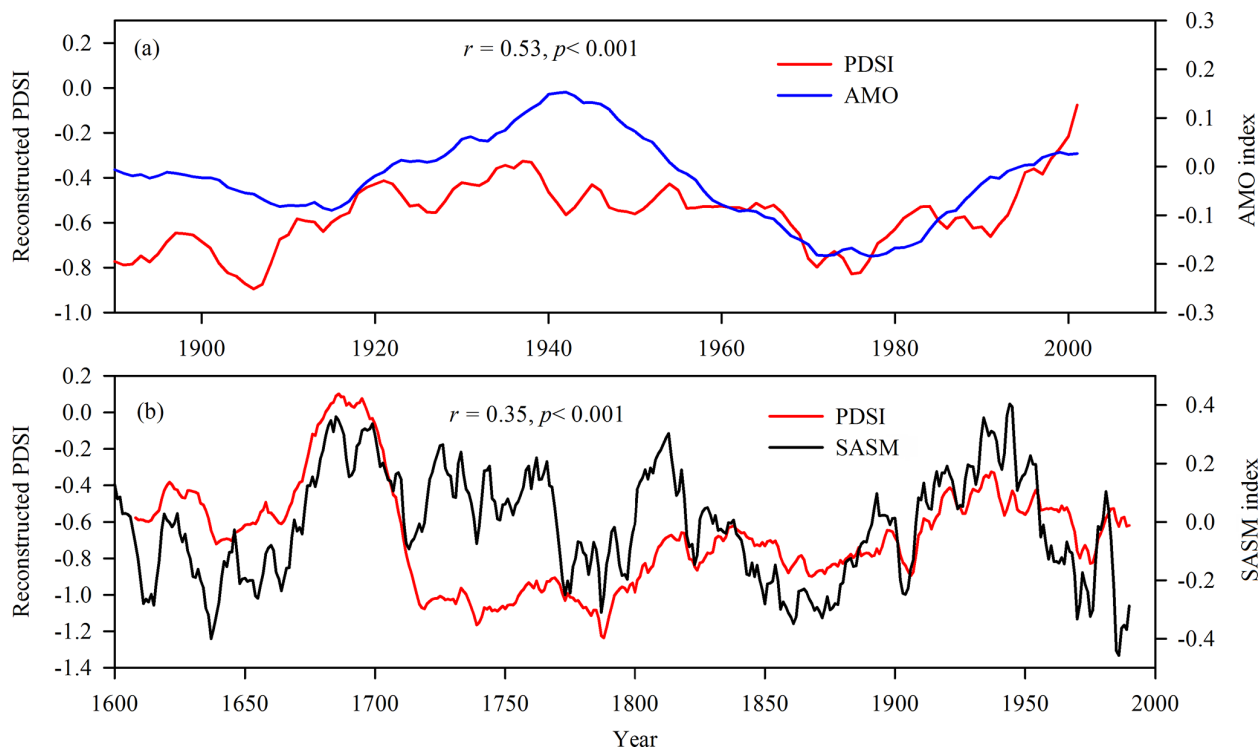

Figure 9. (a) Comparison of the 31-year moving average series between the reconstructed Mar–Aug scPDSI and the AMO index during the common period (1890–2001; van Oldenborgh et al., 2009); **(b)** comparison of the 31-year moving average series between the reconstructed Mar–Aug scPDSI and the South Asian summer monsoon index from June to August (JJA, SASM) (Cook et al., 2010) during the common period (1608–1990).
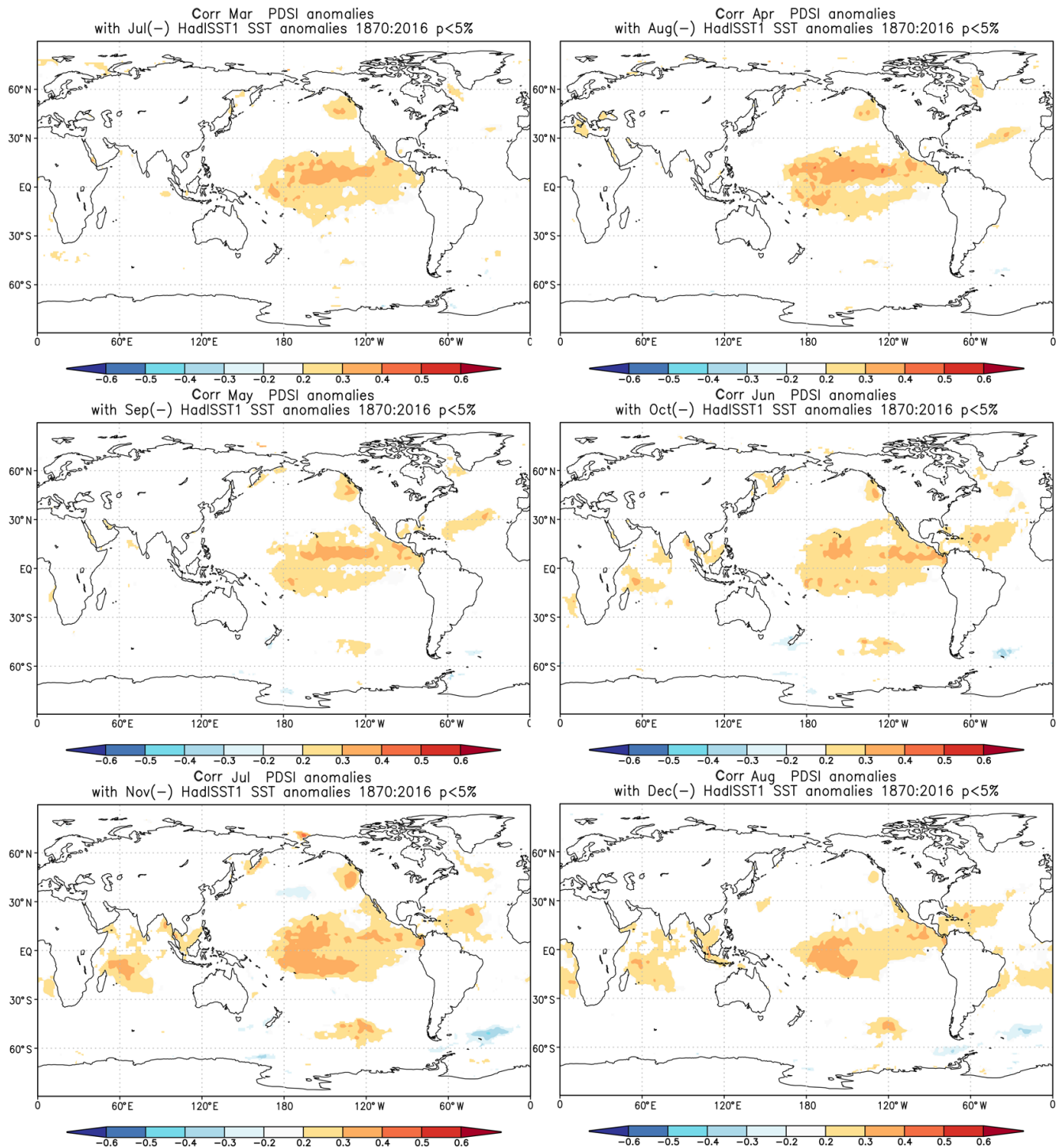
Figure 10. The field correlation between the monthly HadISST1 sea surface temperature and reconstructed PDSI with a lag of 8 months calculated by the KNMI Climate Explorer (1870–2016). The contours with $p > 0.05$ were masked out.

8 months (Table 2 and Fig. 10), so it further indicated that the water availability in this area may be related to large-scale climate oscillations. There is a lag effect of ENSO on drought in the study area, and the lag time is about 4–11 months. The lags in the ENSO impact are very complex and different in different regions (Vicente-Serrano et al., 2011). Therefore, the decrease in drought in our study area may be linked to the enhancement of ENSO activity. However, Khan et al. (2013) showed that most of northern Pakistan is in the monsoon shadow zone, and the Asian monsoon showed an overall

Table 2. Correlation coefficients (r) and p values between the monthly ENSO index and the reconstructed PDSI with a lag of 8 months calculated by the KNMI Climate Explorer.

PDSI Month	ENSO Month	NINO3		NINO3.4		NINO4	
		r	p	r	p	r	p
Jan	May	0.19	0.0445	0.21	0.0270	0.26	0.0063
Feb	Jun	0.23	0.0156	0.26	0.0053	0.28	0.0028
Mar	Jul	0.25	0.0094	0.28	0.0030	0.27	0.0043
Apr	Aug	0.22	0.0226	0.25	0.0083	0.26	0.0087
May	Sep	0.22	0.0202	0.26	0.0074	0.28	0.0045
Jun	Oct	0.18	0.0599	0.24	0.0117	0.29	0.0033
Jul	Nov	0.19	0.0488	0.25	0.0078	0.28	0.0033
Aug	Dec	0.16	0.0773	0.22	0.0157	0.26	0.0049
Sep	Jan	0.20	0.0432	0.24	0.0103	0.26	0.0057
Oct	Feb	0.26	0.0061	0.30	0.0010	0.28	0.0031
Nov	Mar	0.27	0.0038	0.28	0.0020	0.27	0.0040
Dec	Apr	0.25	0.0090	0.27	0.0030	0.31	0.0009

weak trend in recent decades (Wang and Ding, 2006; Ding et al., 2008). Previous studies (Wang et al., 2006; Palmer et al., 2015; Shi et al., 2018; Chen et al., 2019) have confirmed that ENSO is an important factor regulating the hydrological conditions related to the AMO. In the past, severe famine and drought occurred simultaneously with the warm phase of ENSO, and these events were related to the failure of the Indian summer monsoon (Shi et al., 2014).

The middle-frequency cycle (16 years) might have been related to the solar cycle, which is similar to the results of other studies in South Asia (Panthi et al., 2017; Shekhar et al., 2018; Chen et al., 2019). Solar activity may affect climate fluctuations in the HK range in northern Pakistan (Gaire et al., 2017). The low-frequency cycle (36–38 years) might have been caused by the AMO, which is the SST anomaly in the North Atlantic Basin (Fig. 9). Previous studies have shown that the AMO may alter drought or precipitation patterns in North America (Mccabe et al., 2004; Nigam et al., 2011) and Europe (Vicente-Serrano and López-Moreno, 2008). Although our study area is far from the Atlantic Ocean, it may also be affected by the AMO (Lu et al., 2006; Wang et al., 2011; Yadav, 2013). Lu et al. (2006) found that the SST anomalies in the North Atlantic (such as the AMO) can affect the Asian summer monsoon. Goswami et al. (2006) reported the mechanism of the influence of the AMO on Indian monsoon precipitation. The warm AMO appears to cause late withdrawal of the Indian monsoon by strengthening the meridional gradient of the tropospheric temperature in autumn (Goswami et al., 2006; Lu et al., 2006). Yadav (2013) suggested the role of the AMO in modulating winter droughts over the western Himalayas through the tropical Pacific Ocean. Wang et al. (2009) pointed out that the AMO heats the Eurasian middle and upper troposphere in all four seasons, thereby resulting in weakened Asian winter monsoons and enhanced summer monsoons. This is con-

sistent with the finding that the AMO affects the climate in China, which is made possible by the Atlantic–Eurasia wave train from the North Atlantic and is increased owing to global warming (Qian et al., 2014). Further work is still needed to determine the connections between the Pacific and Atlantic oceans and how the two are coupled through the atmosphere and oceans to affect drought in Asia.

Dimri (2006) found that the precipitation surplus in winter from 1958 to 1997 was related to significant heat loss in the northern Arabian Sea, which was mainly due to the intensification of water vapor flow in the west and the enhancement of evaporation. As a result, large-scale changes in Atlantic temperature could also regulate the climate of western Asia. Our result was supported by other dendroclimatic studies (Sano et al., 2005; Chen et al., 2019). Precipitation in the Mediterranean, Black Sea (Giesche et al., 2019), and parts of northern Pakistan showed an upward trend from 1980 to 2010, but precipitation in the HK mountain range was received from the Indian winter monsoon (December–March) and the rain shadows in summer (Khan et al., 2013). Predicting different patterns of the climate cycle is difficult. In addition, the flow of the Upper Indus Basin (UIB) depends on changes in the ablation mass (Rashid et al., 2018; Rao et al., 2018); small changes in the ablation mass may eventually lead to changes in water quality and quantity. The UIB is considered a water tower in the plain (Immerzeel et al., 2010), so the HK mountains are particularly important for extending the proxy network to improve the understanding of different climatic behaviors.

The drought regimes in the HK range in northern Pakistan may be linked to regional, local, and global climate change. We only studied the response of *C. deodara* to different changes in climate in the Chitral region of northern Pakistan. Therefore, we suggest that further high-resolution

and well-dated records are needed to augment the dendroclimatic network in the region.

5   Conclusions

Based on the significance of the tree-ring widths of *C. deodara*, we developed a 468-year chronology (1550–2017). Considering that the EPS threshold was greater than 0.85 (>13 trees), we reconstructed the current March–August PDSI from 1593 to 2016. Our reconstruction captured different drought changes at different timescales in the HK range, Pakistan. Three historic mega-drought events, namely the Strange Parallels Drought (1756–1768), East India Drought (1790–1796), and Late Victorian Great Drought (1876–1878), were captured by our reconstructed PDSI. These large-scale and small-scale droughts might have been caused by cold or hot climate. Our results are consistent with other dendroclimatic records, which further supports the feasibility of our reconstruction. In addition, owing to the different climate change patterns in the region, we suggest extending the different proxy networks to understand the remote teleconnection across the continent on multidecadal to centennial timescales to meet future climate challenges.

References

Abatzoglou, J. T. and Williams, A. P.: Impact of anthropogenic climate change on wildfire across western US forests, P. Natl. Acad. Sci. USA, 113, 11770–11775, 2016.

Ahmad, S., Hussain, Z., Qureshi, A. S., Majeed, R., and Saleem, M.: Drought mitigation in Pakistan: current status and options for future strategies, Working Paper 85, International Water Management Institute, Colombo, Sri Lanka, 2004.

Ahmed, M., Wahab, M., and Khan, N.: Dendroclimatic investigation in Pakistan using *Picea smithiana* (Wall) Boiss – Preliminary results, Pak. J. Bot., 41, 2427–2435, 2009.

Ahmed, M., Wahab, M., Khan, N., Palmer, J., Nazim, K., Khan, M. U., and Siddiqui, M. F.: Some preliminary results of climatic studies based on two pine tree species of Himalayan areas of Pakistan, Pak. J. Bot., 42, 731–738, 2010a.

Ahmed, M., Khan, N., and Wahab, M.: Climate response function analysis of *Abies pindrow* (Royle) Spach. Preliminary results, Pak. J. Bot., 42, 165–171, 2010b.

Ahmed, M., Palmer, J., Khan, N., Wahab, M., Fenwick, P., Esper, J., and Cook, E. D.: The dendroclimatic potential of conifers from northern Pakistan, Dendrochronologia, 29, 77–88, 2011a.

Ahmed, M., Shaukat, S. S., and Siddiqui, M. F.: A multivariate analysis of the vegetation of *Cedrus deodara* forests in Hindu Kush and Himalayan ranges of Pakistan: evaluating the structure and dynamics, Turk. J. Bot., 35, 419–438, 2011b.

Akbar, M., Ali, S., Hyder, S., Ali, M., Begum, F., and Raza, G.: Growth-climate correlation of Himalayan pine (*Pinus wallichiana*) from Ganji forest Skardu districts of Gilgit-Baltistan, Pakistan, Journal of Biodiversity and Environmental Sciences, 5, 405–412, 2014.

Asad, F., Zhu, H., Liang, E., Ali, M., Hamayun, M., Sigdel, S. R., Khalid, M., and Hussain, I.: Climatic signal in tree-ring width chronologies of *Pinus wallichiana* from the Karakoram Mountains in Northern Pakistan, Pak. J. Bot., 49, 2465–2473, 2017a.

Asad, F., Zhu, H., Zhang, H., Liang, E., Muhammad, S., Farhan, S. B., Hussain, I., Wazir, M. A., Ahmed, M., and Esper, J.: Are Karakoram temperatures out of phase compared to hemispheric trends?, Clim. Dynam., 48, 3381–3390, 2017b.

Asad, F., Zhu, H., Jan, F., Yaseen, T., Khan, A., and Khalid, M.: Growth response of *Pinus wallichiana* to climatic factors from the Chiraah Karakoram region, Northern Pakistan, Pak. J. Bot., 50, 1805–1810, 2018.

Bajracharya, A. R., Bajracharya, S. R., Shrestha, A. B., and Maharjan, S. B.: Climate change impact assessment on the hydrological regime of the Kaligandaki Basin, Nepal, Sci. Total Environ., 625, 837–848, 2018.

Betzler, C., Eberli, G. P., Kroon, D., Wright, J. D., Swart, P. K., Nath, B. N., Alvarez-Zarikian, C. A., Alonso-García, M., Bialik, O. M., and Blättler, C. L.: The abrupt onset of the

modern South Asian Monsoon winds, Sci. Rep., 6, 29838, https://doi.org/10.1038/srep29838, 2016.

Bilham, R., Pant, G. B., and Jacoby G. C.: Dendroclimatic potential of Juniper trees from the Sir Sar Range in the Karakoram, Man and Environment, 7, 45–50, 1983.

Borgaonkar, H., Pant, G., and Rupa Kumar, K.: Ring-width variations in *Cedrus deodara* and its climatic response over the western Himalaya, Int. J. Climatol., 16, 1409–1422, 1996.

Bothe, O., Wagner, S., and Zorita, E.: Inconsistencies between observed, reconstructed, and simulated precipitation indices for England since the year 1650 CE, Clim. Past, 15, 307–334, https://doi.org/10.5194/cp-15-307-2019, 2019.

Cannon, F., Carvalho, L. M. V., Jones, C., and Bookhagen, B.: Multi-annual variations in winter westerly disturbance activity affecting the Himalaya, Clim. Dynam., 44, 441–455, 2015.

Chen, F., Zhang, T., Seim, A., Yu, S., Zhang, R., Linderholm, H. W., Kobuliev, Z. V., Ahmadov, A., and Kodirov, A.: Juniper tree-ring data from the Kuramin Range (northern Tajikistan) reveals changing summer drought signals in western Central Asia, Forests, 10, 505, https://doi.org/10.3390/f10060505, 2019.

Cook, E. R. and Kairiukstis, L. A.: Methods of dendrochronology: applications in the environmental sciences, Kuluwer Academic Publishers, Dordrecht, USA, 1990.

Cook, E. R., Meko, D. M., Stahle, D. W., and Cleaveland, M. K.: Drough reconstruction for the continental United States, J. Climate, 12, 1145–1162, 1999.

Cook, E. R., Krusic, P. J., and Jones, P. D.: Dendroclimatic signals in long tree-ring chronologies from the Himalayas of Nepal, Int. J. Climatol., 23, 707–732, 2003.

Cook, E. R., Anchukaitis, K. J., Buckley, B. M., D'Arrigo, R. D., Jacoby, G. C., and Wright, W. E.: Asian monsoon failure and megadrought during the last millennium, Science, 328, 486–489, 2010.

Dimri, A.: Surface and upper air fields during extreme winter precipitation over the western Himalayas, Pure Appl. Geophys., 163, 1679–1698, 2006.

Ding, Y., Wang, Z., and Sun, Y.: Inter-decadal variation of the summer precipitation in East China and its association with decreasing Asian summer monsoon. Part I: Observed evidences, Int. J. Climatol., 28, 1139–1161, 2008.

Esper, J.: Long-term tree-ring variations in Juniperus at the upper timber-line in the Karakorum (Pakistan), The Holocene, 10, 253–260, 2000.

Esper, J., Bosshard, A., Schweingruber, F. H., and Winiger, M.: Tree-rings from the upper timberline in the Karakorum as climatic indicators for the last 1000 years, Dendrochronologia, 13, 79–88, 1995.

Esper, J., Treydte, K., Gärtner, H., and Neuwirth, B.: A tree ring reconstruction of climatic extreme years since 1427 AD for Western Central Asia, Palaeobotanist, 50, 141–152, 2001.

Esper, J., Schweingruber, F. H., and Winiger, M.: 1300 years of climatic history for Western Central Asia inferred from tree-rings, The Holocene, 12, 267-277, 2002.

Esper, J., Shiyatov, S., Mazepa, V., Wilson, R., Graybill, D., and Funkhouser, G.: Temperature-sensitive Tien Shan tree ring chronologies show multi-centennial growth trends, Clim. Dynam., 21, 699–706, 2003.

Esper, J., Krusic, P. J., Ljungqvist, F. C., Luterbacher, J., Carrer, M., Cook, E., Davi, N. K., Hartl-Meier, C., Kirdyanov, A., and Kon-

ter, O.: Ranking of tree-ring based temperature reconstructions of the past millennium, Quaternary Sci. Rev., 145, 134–151, 2016.

Ficklin, D. L., Maxwell, J. T., Letsinger, S. L., and Gholizadeh, H.: A climatic deconstruction of recent drought trends in the United States, Environ. Res. Lett., 10, 044009, https://doi.org/10.1088/1748-9326/10/4/044009, 2015.

Fritts, H. C.: Tree rings and climate, Academic Press, New York, USA, 1976.

Gaire, N. P., Bhuju, D. R., Koirala, M., Shah, S. K., Carrer, M., and Timilsena, R.: Tree-ring based spring precipitation reconstruction in western Nepal Himalaya since AD 1840, Dendrochronologia, 42, 21–30, 2017.

Gaire, N. P., Dhakal, Y. R., Shah, S. K., Fan, Z.-X., Bräuning, A., Thapa, U. K., Bhandari, S., Aryal, S., and Bhuju, D. R.: Drought (scPDSI) reconstruction of trans-himalayan region of central himalaya using *Pinus wallichiana* tree-rings, Palaeogr. Palaeocl., 514, 251–264, 2019.

Giesche, A., Staubwasser, M., Petrie, C. A., and Hodell, D. A.: Indian winter and summer monsoon strength over the 4.2 ka BP event in foraminifer isotope records from the Indus River delta in the Arabian Sea, Clim. Past, 15, 73–90, https://doi.org/10.5194/cp-15-73-2019, 2019.

Goodman, S. J., Blakeslee, R., Christian, H., Koshak, W., Bailey, J., Hall, J., McCaul, E., Buechler, D., Darden, C., and Burks, J.: The North Alabama lightning mapping array: Recent severe storm observations and future prospects, Atmos. Res., 76, 423–437, 2005.

Goswami, B. N., Madhusoodanan, M. S., Neema, C. P., and Sengupta, D.: A physical mechanism for North Atlantic SST influence on the Indian summer monsoon, Geophys. Res. Lett., 33, L02706, https://doi.org/10.1029/2005GL024803, 2006.

Harris, I., Jones, P. D., Osborn, T. J., and Lister, D. H.: Updated high-resolution grids of monthly climatic observations – the CRU TS3. 10 Dataset, Int. J. Climatol., 34, 623–642, 2014.

Hartl-Meier, C., Büntgen, U., Smerdon, J. E., Zorita, E., Krusic, P. J., Ljungqvist, F. C., Schneider, L., and Esper, J.: Temperature covariance in tree ring reconstructions and model simulations over the past millennium, Geophys. Res. Lett., 44, 9458–9469, 2017.

He, M., Bräuning, A., Grießinger, J., Hochreuther, P., and Wernicke, J.: May–June drought reconstruction over the past 821 years on the south-central Tibetan Plateau derived from tree-ring width series, Dendrochronologia, 47, 48–57, 2018.

Hellmann, L., Agafonov, L., Ljungqvist, F. C., Churakova, O., Düthorn, E., Esper, J., Hülsmann, L., Kirdyanov, A. V., Moiseev, P., and Myglan, V. S.: Diverse growth trends and climate responses across Eurasia's boreal forest, Environ. Res. Lett., 11, 074021, https://doi.org/10.1088/1748-9326/11/7/074021, 2016.

Hoerling, M. and Kumar, A.: The perfect ocean for drought, Science, 299, 691–694, 2003.

Holmes, R.: Computer assisted quality control, Tree-ring Bulletin, 43, 69–78, 1983.

Immerzeel, W. W., van Beek, L. P., and Bierkens, M. F.: Climate change will affect the Asian water towers, Science, 328, 1382–1385, 2010.

Immerzeel, W. W., Pellicciotti, F., and Bierkens, M. F. P.: Rising river flows throughout the twenty-first century in two Himalayan glacierized watersheds, Nat. Geosci., 6, 742–745, 2013.

IPCC, Stocker, T. F., Qin, D., Plattner, G. K., Tignor, M., Allen, S. K., Boschung, J., Nauels, A., Xia, Y., Bex, V., Midgley, P. M.

(Eds.) and The Physical Science Basis: Climate change, Contribution of Working Group I to the Fifth Assessment Report of the Intergovernmental Panel on Climate Change, Cambridge University Press, Cambridge and New York, 2013

Kazmi, D. H., Li, J., Rasul, G., Tong, J., Ali, G., Cheema, S. B., Liu, L., Gemmer, M., and Fischer, T.: Statistical downscaling and future scenario generation of temperatures for Pakistan region, Theor. Appl. Climatol., 120, 341–350, 2015.

Khan, N., Ahmed, M., Wahab, M., and Ajaib, M.: Phytosociology, structure and physiochemical analysis of soil in *Quercus baloot* griff, forest district Chitral, Pakistan, Pak. J. Bot., 42, 2429–2441, 2010.

Khan, N., Ahmed, M., and Shaukat, S.: Climatic signal in tree-ring chronologies of *Cedrus deodara* from Chitral HinduKush Range of Pakistan, Geochronometria, 40, 195–207, 2013.

Khan, A., Chen, F., Ahmed, M., and Zafar, M. U.: Rainfall reconstruction for the Karakoram region in Pakistan since 1540 CE reveals out-of-phase relationship in rainfall between the southern and northern slopes of the Hindukush-Karakorum-Western Himalaya region, Int. J. Climatol., 40, 52–62, 2019.

Klippel, L., Krusic, P. J., Brandes, R., Hartl-Meier, C., Trouet, V., Meko, M., and Esper, J.: High-elevation inter-site differences in Mount Smolikas tree-ring width data, Dendrochronologia, 44, 164–173, 2017.

Lesk, C., Rowhani, P., and Ramankutty, N.: Influence of extreme weather disasters on global crop rproduction, Nature, 529, 84–87, 2016.

Li, Q., Liu, Y., Song, H., Yang, Y., and Zhao, B.: Divergence of tree-ring-based drought reconstruction between the individual sampling site and the Monsoon Asia Drought Atlas: an example from Guancen Mountain, Sci. Bull., 60, 1688–1697, 2015.

Liu, Y., Shishov, V., Shi, J., Vaganov, E., Sun, J., Cai, Q., Djanseitov, I., and An, Z.: The forecast of seasonal precipitation trend at the north Helan Mountain and Baiyinaobao regions, Inner Mongolia for the next 20 years, Chinese Sci. Bull., 49, 410–415, 2004.

Lu, R., Dong, B., and Ding, H.: Impact of the Atlantic Multidecadal Oscillation on the Asian summer monsoon, Geophys. Res. Lett., 33, 194–199, 2006.

Lutz, A. F., Immerzeel, W. W., Shrestha, A. B., and Bierkens, M. F. P.: Consistent increase in high Asia's runoff due to increasing glacier melt and precipitation, Nat. Clim. Change, 4, 587, https://doi.org/10.1038/nclimate2237, 2014.

Malik, A., Brönnimann, S., Stickler, A., Raible, C. C., Muthers, S., Anet, J., Rozanov, E., and Schmutz, W.: Decadal to multi-decadal scale variability of Indian summer monsoon rainfall in the coupled ocean-atmosphere-chemistry climate model SOCOL-MPIOM, Clim. Dynam., 49, 3551–3572, 2017.

Mann, M. E. and Lees, J. M.: Robust estimation of background noise and signal detection in climatic time series, Clim. Change, 33, 409–445, 1996.

Martínez-Vilalta, J. and Lloret, F.: Drought-induced vegetation shifts in terrestrial ecosystems: the key role of regeneration dynamics, Global Planet. Change, 144, 94–108, 2016.

Mccabe, G. J., Palecki, M. A., and Betancourt, J. L.: Pacific and Atlantic Ocean influences on multidecadal drought frequency in the United States, P. Natl. Acad. Sci. USA, 101, 4136–4141, 2004.

McDowell, N., Brooks, J. R., Fitzgerald, S., and Bond, B. J.: Carbon isotope discrimination and growth response to stand density reductions in old *Pinus ponderosa* trees, presented at 3rd International Conference on Applications of Stable isotope Techniques to Ecological Studies, Flagstaff, AZ, 29 April–1 May 2002.

Miyan, M. A.: Droughts in Asian least developed countries: vulnerability and sustainability, Weather and Climate Extremes, 7, 8–23, 2015.

Nigam, S., Guan, B., and Ruiz-Barradas, A.: Key role of the Atlantic Multidecadal Oscillation in 20th century drought and wet periods over the Great Plains, Geophys. Res. Lett., 38, 239–255, 2011.

NOAA: International Tree-Ring Data Bank, available at: https://www.ncdc.noaa.gov/paleo-search/?dataTypeId=18, last access: 24 April 2020.

Palmer, J. G., Cook, E. R., Turney, C. S., Allen, K., Fenwick, P., Cook, B. I., O'Donnell, A., Lough, J., Grierson, P., and Baker, P.: Drought variability in the eastern Australia and New Zealand summer drought atlas (ANZDA, CE 1500–2012) modulated by the Interdecadal Pacific Oscillation, Environ. Res. Lett., 10, 124002, https://doi.org/10.1088/1748-9326/10/12/124002, 2015.

Panthi, S., Bräuning, A., Zhou, Z.-K., and Fan, Z.-X.: Tree rings reveal recent intensified spring drought in the central Himalaya, Nepal, Global Planet. Change, 157, 26–34, 2017.

Pepin, N., Bradley, R., Diaz, H., Baraer, M., Caceres, E., Forsythe, N., Fowler, H., Greenwood G, Hashmi, M. Z., Liu, X. D., Miller, J. R., Ning, L., Ohmura, A., Palazzi, E., Rangwala, I., Schöner, W., Severskiy, I., Shahgedanova, M., Wang, M. B., Williamson, S. N., and Yang D. Q.: Elevation-dependent warming in mountain regions of the world, Nat. Clim. Change, 5, 424–430, 2015.

Qian, C., Yu, J., and Chen, G.: Decadal summer drought frequency in China: the increasing influence of the Atlantic Multi-decadal Oscillation, Environ. Res. Lett. 9, 124004, https://doi.org/10.1088/1748-9326/9/12/124004, 2014.

Rao, M. P., Cook, E. R., Cook, B. I., Palmer, J. G., Uriarte, M., Devineni, N., Lall, U., D'Arrigo, R. D., Woodhouse, C. A., and Ahmed, M.: Six centuries of upper Indus Basin streamflow variability and its climatic drivers, Water Resour. Res., 54, 5687–5701, 2018.

Rashid, M. U., Latif, A., and Azmat, M.: Optimizing irrigation deficit of multipurpose Cascade reservoirs, Water Resour. Manage., 32, 1675–1687, 2018.

Rasul, G.: Food, water, and energy security in South Asia: A nexus perspective from the Hindu Kush Himalayan region, Environ. Sci. Policy, 39, 35–48, 2014.

Sano, M., Furuta, F., Kobayashi, O., and Sweda, T.: Temperature variations since the mid-18th century for western Nepal, as reconstructed from tree-ring width and density of Abies spectabilis, Dendrochronologia, 23, 83–92, 2005.

Shekhar, M.: Application of multi proxy tree ring parameters in the reconstruction of climate vis-à-vis glacial fluctuations from the eastern Himalaya, University of Lucknow, Lucknow, India, 2015.

Shekhar, M., Pal, A. K., Bhattacharyya, A., Ranhotra, P. S., and Roy, I.: Tree-ring based reconstruction of winter drought since 1767 CE from Uttarkashi, Western Himalaya, Quatern. Int., 479, 58–69, 2018.

Shi, C., Shen, M., Wu, X., Cheng, X., Li, X., Fan, T., Li, Z., Zhang, Y., Fan, Z., and Shi, F.: Growth response of alpine treeline forests to a warmer and drier climate on the southeastern Tibetan Plateau, Agr. Forest Meteorol., 264, 73–79, 2019.

Shi, F., Li, J., and Wilson, R. J.: A tree-ring reconstruction of the South Asian summer monsoon index over the past millennium, Sci. Rep., 4, 6739, https://doi.org/10.1038/srep06739, 2014.

Shi, H., Wang, B., Cook, E. R., Liu, J., and Liu, F.: Asian summer precipitation over the past 544 years reconstructed by merging tree rings and historical documentary records, J. Climate, 31, 7845–7861, 2018.

Sigdel, M. and Ikeda, M.: Spatial and temporal analysis of drought in Nepal using standardized precipitation index and its relationship with climate indices, Journal of Hydrology and Meteorology, 7, 59–74, 2010.

Singh, J., Park, W. K., and Yadav, R. R.: Tree-ring-based hydrological records for western Himalaya, India, since AD 1560, Clim. Dynam., 26, 295–303, 2006.

Sinha, A., Cannariato, K. G., Stott, L. D., Cheng, H., Edwards, R. L., Yadava, M. G., Ramesh, R., and Singh, I. B.: A 900-year (600 to 1500 AD) record of the Indian summer monsoon precipitation from the core monsoon zone of India, Geophys. Res. Lett., 34, L16707, https://doi.org/10.1029/2007GL030431, 2007.

Sinha, A., Berkelhammer, M., Stott, L., Mudelsee, M., Cheng, H., and Biswas, J.: The leading mode of Indian Summer Monsoon precipitation variability during the last millennium, Geophys. Res. Lett., 38, L15703, https://doi.org/10.1029/2011GL047713, 2011.

Stokes, M. A. and Smiley, T. L.: An introduction to tree-ring dating, University of Arizona Press, Tucson, USA, 1968.

Sun, C. and Liu, Y.: Tree-ring-based drought variability in the eastern region of the Silk Road and its linkages to the Pacific Ocean, Ecol. Indic., 96, 421–429, 2019.

Tejedor, E., Saz, M., Esper, J., Cuadrat, J., and de Luis, M.: Summer drought reconstruction in northeastern Spain inferred from a tree ring latewood network since 1734, Geophys. Res. Lett., 44, 8492–8500, 2017.

Trenberth, K. E., Dai, A., van der Schrier, G., Jones, P. D., Barichivich, J., Briffa, K. R., and Sheffield, J.: Global warming and changes in drought, Nat. Clim. Change, 4, 17–22, 2014.

Treydte, K. S., Schleser, G. H., Helle, G., Frank, D. C., Winiger, M., Haug, G. H., and Esper, J.: The twentieth century was the wettest period in northern Pakistan over the past millennium, Nature, 440, 1179–1182, 2006.

van der Schrier, G., Barichivich, J., Briffa, K., and Jones, P.: A scPDSI-based global data set of dry and wet spells for 1901–2009, J. Geophys. Res.-Atmos., 118, 4025–4048, 2013.

van Oldenborgh, G. J. and Burgers, G.: Searching for decadal variations in ENSO precipitation teleconnections, Geophys. Res. Lett., 32, L15701, https://doi.org/10.1029/2005GL023110, 2005.

van Oldenborgh, G. J., te Raa, L. A., Dijkstra, H. A., and Philip, S. Y.: Frequency- or amplitude-dependent effects of the Atlantic meridional overturning on the tropical Pacific Ocean, Ocean Sci., 5, 293–301, https://doi.org/10.5194/os-5-293-2009, 2009.

Vicente-Serrano, S. M. and López-Moreno, J. I.: Nonstationary influence of the North Atlantic Oscillation on European precipitation, J. Geophys. Res.-Atmos., 113, D20120, https://doi.org/10.1029/2008JD010382, 2008.

Vicente-Serrano, S. M., López-Moreno, J. I., Gimeno, L., Nieto, R., Morán-Tejeda, E., Lorenzo-Lacruz, J., Beguería, S., and Azorin-Molina, C.: A multiscalar global evaluation of the impact of ENSO on droughts, J. Geophys. Res.-Atmos., 116, D20109, https://doi.org/10.1029/2011JD016039, 2011.

Wang, B. and Ding, Q.: Changes in global monsoon precipitation over the past 56 years, Geophys. Res. Lett., 33, L06711, https://doi.org/10.1029/2005GL025347, 2006.

Wang, B., Ding, Q., and Jhun, J. G.: Trends in Seoul (1778–2004) summer precipitation, Geophys. Res. Lett., 33, L15803, https://doi.org/10.1029/2006GL026418, 2006.

Wang, H., Chen, F., Ermenbaev, B., and Satylkanov, R.: Comparison of drought-sensitive tree-ring records from the Tien Shan of Kyrgyzstan and Xinjiang (China) during the last six centuries, Advances in Climate Change Research, 8, 18–25, 2017.

Wang, Y., Li, S., and Luo, D.: Seasonal response of Asian monsoonal climate to the Atlantic Mutidecadal Oscillation, J. Geophys. Res.-Atmos. 114, D02112, https://doi.org/10.1029/2008JD010929, 2009.

Wang, X., Zhang, Q., Ma, K., and Xiao, S.: A tree-ring record of 500-year dry-wet changes in northern Tibet, China, Holocene, 18, 579–588, 2008.

Wang, X., Brown, P. M., Zhang, Y., and Song, L.: Imprint of the Atlantic multidecadal oscillation on tree-ring widths in northeastern Asia since 1568, PLOS ONE, 6, e22740, https://doi.org/10.1371/journal.pone.0022740, 2011.

Wei, W. and Lohmann, G.: Simulated Atlantic multidecadal oscillation during the Holocene, J. Climate, 25, 6989–7002, 2012.

Wigley, T. M., Briffa, K. R., and Jones, P. D.: On the average value of correlated time series, with applications in dendroclimatology and hydrometeorology, J. Clim. Appl. Meteorol., 23, 201–213, 1984.

Wiles, G. C., Solomina, O., D'Arrigo, R., Anchukaitis, K. J., Gensiarovsky, Y. V., and Wiesenberg, N.: Reconstructed summer temperatures over the last 400 years based on larch ring widths: Sakhalin Island, Russian Far East, Clim. Dynam., 45, 397–405, 2015.

Xu, C., Sano, M., Dimri, A. P., Ramesh, R., Nakatsuka, T., Shi, F., and Guo, Z.: Decreasing Indian summer monsoon on the northern Indian sub-continent during the last 180 years: evidence from five tree-ring cellulose oxygen isotope chronologies, Clim. Past, 14, 653–664, https://doi.org/10.5194/cp-14-653-2018, 2018.

Yadav, R. R.: Tree ring evidence of a 20th century precipitation surge in the monsoon shadow zone of the western Himalaya, India, J. Geophys. Res.-Atmos., 116, D02112, https://doi.org/10.1029/2010JD014647, 2011.

Yadav, R. R.: Tree ring–based seven-century drought records for the Western Himalaya, India, J. Geophys. Res.-Atmos., 118, 4318–4325, 2013.

Yadav, R. R. and Bhutiyani, M. R.: Tree-ring-based snowfall record for cold arid western Himalaya, India since AD 1460, J. Geophsy. Res.-Atmos., 118, 7516–7522, 2013.

Yadav, R. R., Gupta, A. K., Kotlia, B. S., Singh, V., Misra, K. G., Yadava, A. K., and Singh, A. K.: Recent wetting and glacier expansion in the northwest Himalaya and Karakoram, Sci. Rep., 7, 6139, https://doi.org/10.1038/s41598-017-06388-5, 2017.

Yao, J. and Chen, Y.: Trend analysis of temperature and precipitation in the Syr Darya Basin in Central Asia, Theor. Appl. Climatol., 120, 521–531, 2015.

Yaqub, M., Eren, B., and Doğan, E.: Flood causes, consequences and protection measures in Pakistan, Disaster Science and Engineering, 1, 8–16, 2015.

Yu, J., Shah, S., Zhou, G., Xu, Z., and Liu, Q.: Tree-ring-recorded drought variability in the northern Dax-

ing'anling Mountains of northeastern China, Forests, 9, 674, https://doi.org/10.3390/f9110674, 2018.

Yu, M., Li, Q., Hayes, M. J., Svoboda, M. D., and Heim, R. R.: Are droughts becoming more frequent or severe in China based on the standardized precipitation evapotranspiration index: 1951–2010?, Int. J. Climatol., 34, 545–558, 2014.

Zafar, M. U., Ahmed, M., Farooq, M. A., Akbar, M., and Hussain, A.: Standardized tree ring chronologies of *Picea smithiana* from two new sites of northern area Pakistan, World Applied Sciences Journal, 11, 1531–1536, 2010.

Zang, C. and Biondi, F.: Treeclim: an R package for the numerical calibration of proxy-climate relationships, Ecography, 38, 431–436, 2015.

Zhang, Q.-B., Evans, M. N., and Lyu, L.: Moisture dipole over the Tibetan Plateau during the past five and a half centuries, Nat. Commun., 6, 8062, https://doi.org/10.1038/ncomms9062, 2015.

Zhu, L., Li, Z., Zhang, Y., and Wang, X.: A 211-year growing season temperature reconstruction using tree-ring width in Zhangguangcai Mountains, Northeast China: linkages to the Pacific and Atlantic Oceans, Int. J. Climatol., 37, 3145–3153, 2017.